ARCHIVES OF ELECTRICAL ENGINEERING VOL. 69(1), pp. 69–88 (2020)

DOI 10.24425/aee.2020.131759

Multi motor neural PID relative coupling speed synchronous control

YONGLONG ZHANG[1], YUEJUN AN[1], GUANGYU WANG[2], XIANGLING KONG[2]

[1] *School of Electrical Engineering*
Shenyang University of Technology
Shenyang, 110870, China

[2] *Vacuum Dry Pump Business Division*
SKY Technology Development Co. Ltd
Chinese Academy of Sciences
Shenyang, 110179, China
e-mail: 1131470120@qq.com

(Received: 05.09.2019, revised: 19.10.2019)

Abstract: When the traditional multi-motor speed synchronous control strategy is applied to the vacuum pump system, it is prone to the drawbacks of large synchronization error. In this paper, a simplified mathematical model of the motor for a vacuum pump is established and the transfer function is introduced, which weakens the multivariable, strong coupling and nonlinear characteristics of the motor system. According to the basic principle of the relative coupling control strategy, the neural network Proportion Integration Differentiation (PID) is introduced as a speed compensator in this system. It effectively improves the synchronization and anti-interference ability of the multi motor.

Key words: fuzzy control, multi motor synchronous control, neural PID, relative coupling control, vacuum pump

1. Introduction

With the continuous development of vacuum application technology, the demand for vacuum pump in the field of large-scale integrated circuit manufacturing equipment industry, electric vacuum technology, a high-energy particle accelerator, surface science and material manufacturing is increasing. The vacuum pump usually consists of two parts: the mechanical part and the drive motor. The design and control of the drive motor has been a hot topic of scholars.

However, when the vacuum pump is loaded for a long time, the mechanical meshing between the multiple gears increases the gear clearance, which may affect the life of the vacuum pump. For this reason, it is important to research the multi-motor synchronous control of the vacuum pump.

At present, the multi-motor synchronous control strategies contains main order control, master-slave control, cross coupling control, ring coupling control, virtual line shaft control, and relative coupling control. [1] presented the application of an "electronic line-shafting" control technique which serves to replicate and even improve the historical, mechanical line-shafted properties. However, it has the disadvantage of large closed-loop length of the system that results in long adjustment time in the presence of disturbances. Based on the master-slave control, some optimization and improvement have been done [2]. However, for the synchronous control of the three motors studied in this paper, its anti-interference ability and synchronization ability still have certain deficiencies, such as being disturbed from the slave motor. While the main motor may not quickly follow the response of the slave motor, the system loses synchronization. [3] proposed a cross-coupling control strategy suitable for two-axis synchronous motion, but when it is extended to the synchronous motion form of three motors, its topology is extremely complicated. [4] took two permanent magnet servo linear motors as the research object, the improved cross-coupling control strategy was used to study the synchronization performance of the two motors under different working conditions. Similarly, the cross-coupling control strategy is difficult to extend to the three-motor synchronous control studied in this paper. [5] took the driving motor for papermaking as the research object, the electronic line-shafting was introduced to replace the traditional rigid connection method, which improved the synchronous running performance of the papermaking system. But the closed-loop adjustment time of this kind of control mode may be long, and for some sudden disturbances, there may be a problem of large synchronization error. The different control methods were introduced and compared, such as cross-coupling control, master-slave control, deviation coupling control, and so on [6], which provides a reference for the selection of the control mode of the three-motor synchronous control system in this paper.

In addition, in order to improve the synchronization performance and anti-interference performance of the system, the researchers have combined intelligent control algorithms with synchronous control strategies and proposed many control schemes suitable for multi-motor speed synchronous control systems. C. Cong combined decoupling technology of the adaptive neuron decoupling compensator, the Radial Basis Function (RBF) neural network adaptive Proportion Integration Differentiation (PID) controller was adopted to design the neural network controller of a two-motor synchronous system [7]. The neural network have good self-learning and nonlinear approximation ability, which may effectively improve the synchronization performance and anti-interference. In order to overcome the time-varying and nonlinear problems of parameters in complex systems, Professor Liu of Jiangsu University have proposed a multi-motor synchronous control strategy based on second-order auto-disturbance rejection control technology in 2012 [8]. It adopts the "separation principle", error feedback and an extended state tracker are independently designed and systematically combined. G. Liu has constructed a neural network generalized inverse system and combined it with a two-motor system [9]. Professor Tingna Shi presents an improved relative coupling control structure for a multi-motor speed synchronous driving system [10]. It introduces an additional speed controller so that all the motors in the system can be

treated as an entity. In order to address the problems of stability and tracking control for a multi-motor servomechanism with unmodeled dynamics, Guofa Sun employs neural active disturbance rejection control to decrease the tracking error and synchronization error [11].

However, the research on the synchronous control of multi motor for vacuum pumps is not thoroughly. There are two main reasons: one is that the vacuum pump motor is in vacuum environment, the motor temperature rise may cause motor parameters to be variable, which will bring challenges to the traditional synchronous control system parameter tuning; the second is that the vacuum pump is susceptible to shock load, which puts higher requirements on the robustness of traditional control systems [12].

For the above reason, compared with other control strategies, the relative coupling control has the advantages of simple structure, easy construction and high anti-interference performance, the neural network PID is introduced as the system speed compensator, which may effectively improve the synchronization performance and anti-interference performance of the multi-motor. With the software of Matlab/Simulink, the neural PID deviation coupling speed synchronization control system of the vacuum pump motor is designed and the theoretical analysis and software simulation is compared with the control effects of the typical control strategy.

The structure of this paper is as follows: after the introduction, in Section 2, the mathematical model for vacuum pump is presented in detail. In Section 3 and Section 4, multi motor relative coupling speed synchronous control with neural PID-fuzzy controller-discrete PID are built, respectively. In Section 5, for different operation conditions, including the load on three motors at different times, and considering the parameter change, such as controller time constant change, the subtle change of motor inertia, the synchronization performance of a multi motor synchronous system is simulated and analyzed.

2. Multi-motor mathematical model for vacuum pump

The neural PID relative coupling speed synchronization control system of the three-motor for a vacuum pump has been designed. This section introduces the basic structure of the vacuum pump and the motor for a vacuum pump and establishes the mathematical model of the multi-motor for a vacuum pump. The Roots pump is a volume vacuum pump. Three shafts of the Roots pump are mounted horizontally in parallel. As shown in Figure 1, the drive shaft drives the driven shafts on both sides via the synchronous gears at the shaft ends, thereby drives the active rotors to mesh with the driven rotors on both sides. Taking Figure 1 as an example, the drive shaft rotates clockwise and the two driven shafts rotate counterclockwise. The position of the gas inlet and exhaust ports is marked in the Figure 1.

In Figure 1, the active rotor and the two driven rotors continuously discharge the gas. At the same time, the three shafts are mechanically engaged by the synchronous gears. But long-term on load operation may cause the gears wear.

Figure 2 is a basic structural diagram of the canned motor for vacuum pump, which mainly includes a stator core, stator winding, stator can, rotor core and rotor bar. The canned motor equivalent circuit for vacuum pump is given in [13].

Referring to this equivalent circuit and equivalent magnetic circuit, a mathematical model of the canned motor can be established. The canned motor in this paper contains a stator can and its

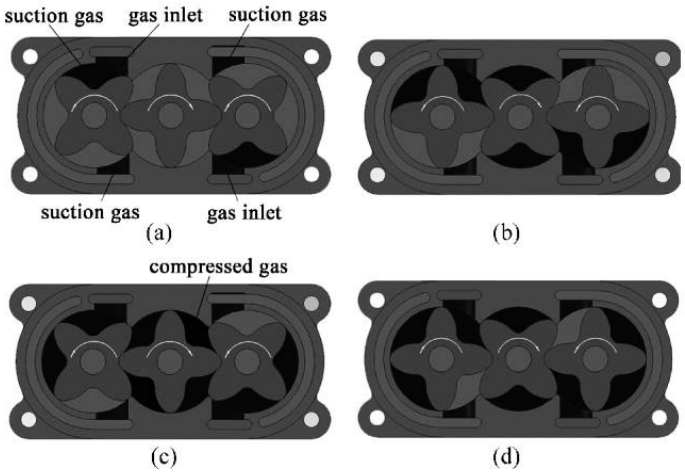

Fig. 1. Structure of a three-axis Roots vacuum pump [6]

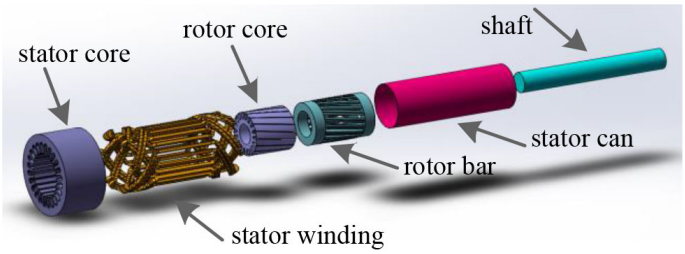

Fig. 2. Canned motor structure diagram for vacuum pump

impedance is:

$$L_{sctot} = L_{sc} + L_m + L_{scm}, \tag{1}$$

where $L_m + L_{scm}$ is the mutual inductance between stator can and stator winding, L_m is the magnetizing inductance. The total inductance of the rotor is L_{rbtot}.

$$L_{rbtot} = L_{rb} + L_m, \tag{2}$$

where L_{rb} is the rotor bar inductance. The subscripts s and r represent the physical quantities of the stator side and rotor side of the motor, respectively. M represents the mutual inductance between stator and rotor. The flux linkage equation is:

$$\begin{bmatrix} \lambda_s \\ \lambda_r \end{bmatrix} = \begin{bmatrix} L_s & M_{sr} \\ M_{rs} & L_r \end{bmatrix} \cdot \begin{bmatrix} I_s \\ I_r \end{bmatrix}, \tag{3}$$

$$[\lambda_s] = \begin{bmatrix} \lambda_{st} \\ \lambda_{sc} \end{bmatrix}, \qquad [\lambda_r] = \begin{bmatrix} 0 \\ \lambda_{rb} \\ \lambda_{rbd} \end{bmatrix}. \tag{4}$$

At the same time, the matrix $[L_s]$ and $[L_r]$ can also be written as:

$$[L_s] = \begin{bmatrix} L_{st} + L_{scm} + L_m & L_{scm} + L_m \\ L_{scm} + L_m & L_{st} + L_{scm} + L_m \end{bmatrix},$$
$$[L_r] = \begin{bmatrix} L_m & L_m & L_m \\ L_m & L_{rb} + L_m & L_m \\ L_m & L_m & L_{rbd} + L_{rbrbd} + L_m \end{bmatrix}. \tag{5}$$

The mutual inductance between the stator and rotor is $[M_{sr}]$:

$$[M_{sr}] = [M_{rs}]^T = \begin{bmatrix} L_m & L_m & L_m \\ L_m & L_m & L_m \end{bmatrix}. \tag{6}$$

The stator current matrix is $[I_s]$, the rotor current matrix is $[I_r]$:

$$[I_s] = \begin{bmatrix} I_{st} \\ I_{sc} \end{bmatrix}, \qquad [I_r] = \begin{bmatrix} 0 \\ I_{rb} \\ I_{rbd} \end{bmatrix}, \tag{7}$$

where L_{st} is the stator leakage inductance, L_m is the excitation inductance, L_{sc} is the stator can leakage inductance, L_{rb} is the rotor bar inductance, L_{rbd} is the rotor body inductance, L_{scm} is the mutual inductance between stator can and air gap, L_{rbrbd} is the mutual inductance between the rotor bar and rotor body.

$$[M_{sr}] = [M_{rs}]^T = \begin{bmatrix} L_m & L_m & L_m \\ L_m & L_m & L_m \end{bmatrix}, \qquad [I_s] = \begin{bmatrix} I_{st} \\ I_{sc} \end{bmatrix}, \qquad [I_r] = \begin{bmatrix} 0 \\ I_{rb} \\ I_{rbd} \end{bmatrix}, \tag{8}$$

The parameters of the canned motor are listed in Table 1.

Table 1. Parameters of the canned motor

Rated power	P_N	2.2	kW
Rated phase current	I_1	5.18	A
Stator phase resistance	R_1	3.05	Ω
Stator leakage reactance	X_1	3.10	Ω
Rotor leakage reactance	X_2	3.77	Ω
Moment of inertia	J	0.0019	kg·m^2
Rated speed	n_N	2950	rpm
Rated torque	T_N	7.59	N·m
Pole pairs	–	1	–
Connection type	–	Wye	–

In order to realize the vector control of the canned motor, the canned motor is often equivalent to a controllable DC motor by mathematical coordinate transformation and then the excitation and the torque component of the current are respectively controlled to achieve high performance control [14–16]. In the process of coordinate transformation, there are phase transformation (3/2 and 2/3 transformation) and rotation transformation ($2s/2r$ and $2r/2s$ transformation). If these transformations are equivalent offsets and small hysteresis of an inverter is ignored, the mathematical model of the canned motor can be expressed in the form of a transfer function [17].

In Figure 3, based on the above deduction and analysis, the speed feedback coefficient α is 9.55, the control signal amplification coefficient K_S is 110, the torque transfer coefficient K_T is 6, the intermediate frequency bandwidth h is 5 (according to the minimum resonance peak principle [18]), K_N is 151.49; τ_n is 0.4449; K_n is 0.00889.

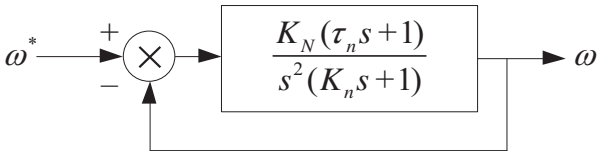

Fig. 3. Mathematical model of canned motor

3. Multi-motor neural PID relative coupling speed synchronization control for vacuum pump

The neural PID relative coupling speed controller designed in this paper is combined three-layer forward neural network with a digital PID algorithm. The digital PID control algorithm is [19–21]:

$$u(k) = K_P\, e(k) + K_I \sum_{0}^{t} e(k) + K_D[e(k) - e(k-1)]. \tag{9}$$

In Equation (9), $u(k)$ is the output of the controller; $e(k)$ is the systematic error; K_P is the proportional coefficient, K_I is the integral coefficient and K_D is differential coefficient.

The input layer has three neurons, received system error, a cumulative error term and differential error term, respectively.

$$\begin{cases} C_P(k) = e(k) \\ C_I(k) = \sum_{0}^{t} e(k) \\ C_D(k) = e(k) - e(k-1) \end{cases}. \tag{10}$$

The input vector $\boldsymbol{X}$ is: $\boldsymbol{X} = [C_P,\ C_I,\ C_D]$.

It should be noted that the number of neurons p is related to the complexity of the system [24]. The input of the j-th neuron in the hidden layer is:

$$net_j(k) = \sum_{i=0}^{3} v_{ij}\, x_i(k), \quad j = 1, 2, \ldots, p. \tag{11}$$

In Equation (11), $x_0(k) = -1$, v_{ij} is the threshold value and y_j^k is the hidden layer output, the activation function is a single polar sigmoid function. The output layer consists of three neurons, K_P, K_I, and K_D. The output vector $\boldsymbol{O}$ is: $\boldsymbol{O} = [K_P,\ K_I,\ K_D]$. The relationship between the output of the entire controller and the output of the neural network is:

$$u(k) = K_P\, C_P + K_I\, C_I + K_D\, K_D\,. \tag{12}$$

S-function is used to code the neural PID that contains seven variables; three discrete state variables; four output variables: the control rate u, proportional, integral and differential coefficient.

The internal structure of the neural PID is shown in Figure 4. It mainly includes an input layer, hidden layer, and output layer. The internal structure block diagram of the overall controller is shown in Figure 5.

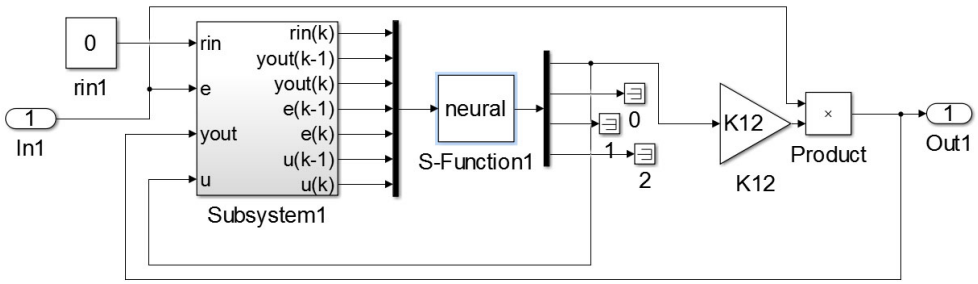

Fig. 4. Internal structure of the neural PID

The fuzzy compensation relative coupling control designed in this paper is based on the principle of conventional relative coupling control. The fuzzy controller is introduced into the speed compensator [22–24]. Among them, the design of the fuzzy controller includes input and output quantization, membership function design, rule formulation and fuzzy domain design [25, 26].

1) The input design of the fuzzy controller: the deviation is e, the rate of change of the deviation is ec, the output is the control quantity u;

2) Design of fuzzy controller domain: the fuzzy domain E of the input error e can be defined as $(-i, -i{+}1, -i{+}2, ..., 0, ..., i{-}2, i{-}1, i)$ [27, 28]. The fuzzy domain EC of the rate of change of the deviation ec can be defined as $(-j, j{+}1, -j{+}2, ..., 0, ..., j{-}2, j{-}1, j)$. Consider that the motor rated speed is 2 950 rpm, in order to reduce the complexity of the fuzzy operation rule, take $i = 6$, $j = 6$; the speed error range is within 20 r/min (upper limit $h_j = 20$, lower limit $l_1 = -20$), the quantization factor K_{e1} of e can be obtained by Equation (13)):

$$K_{e1} = \frac{2i}{h_1 - l_1}\,. \tag{13}$$

Similarly, the change rate ec of the speed error is around 150 (the upper limit $h_2 = 150$, $l_2 = -150$), and the quantization factor K_{e2} of ec can be obtained by Equation (14):

$$K_{e2} = \frac{2i}{h_2 - l_2}\,. \tag{14}$$

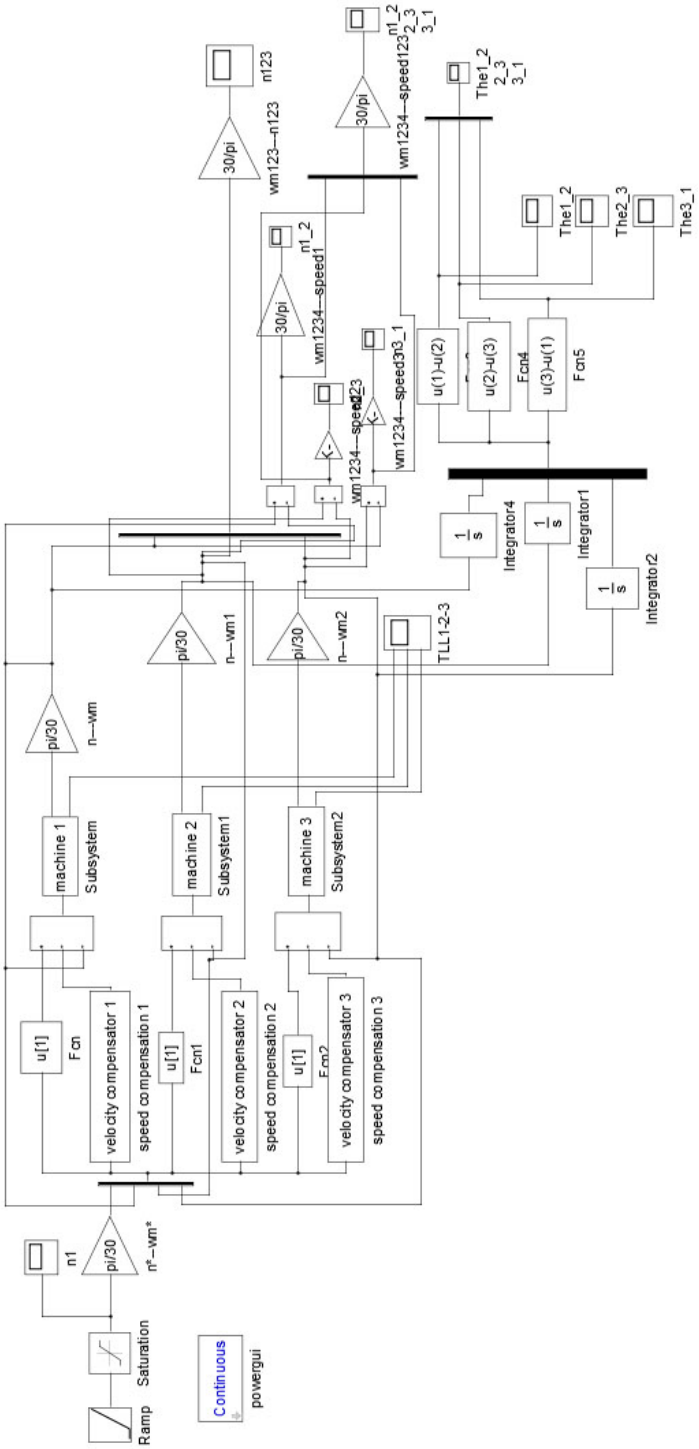

Fig. 5. Internal block diagram of the overall controller

3) Analogous to the input quantization factor, the output quantization factor can be calculated by Equation (15):

$$K_u = \frac{h_3 - l_3}{2k}, \tag{15}$$

where $k = 6$, $h_3 = 200$, $l_3 = -200$.

4) Output design of a fuzzy controller: multiply the output U of the fuzzy domain by the quantization factor K_u to obtain the actual control output [29].

$$u = K_u \cdot U. \tag{16}$$

The range of U is $(-6,\ -5,\ -4,\ -3,\ -2,\ -1,\ 0,\ 1,\ 2,\ 3,\ 4,\ 5,\ 6)$.

5) Design of a fuzzy control rule [30]: The fuzzy rule is listed in Table 2.

Table 2. Fuzzy control rule table

	NB	NM	NS	ZE	PS	PM	PB
NB	NB	NB	NB	NB	NM	ZE	ZE
NM	NB	NB	NB	NB	NS	ZE	ZE
NS	NM	NM	NM	NM	ZE	PS	PS
ZE	NM	NM	NS	ZE	PS	PM	PM
PS	NS	NS	ZE	PS	PM	PM	PM
PM	ZE	ZE	PS	PM	PB	PB	PB
PB	ZE	ZE	PM	PB	PB	PB	PB

The basic structure of the designed fuzzy controller is shown in Figure 6.

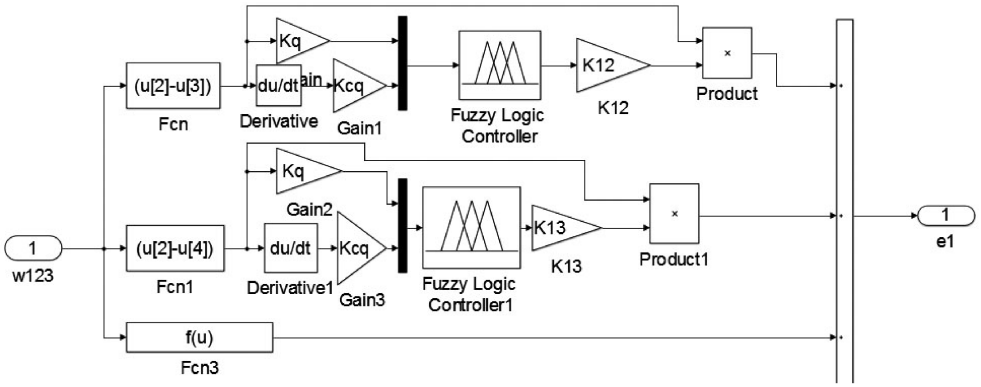

Fig. 6. Basic structure of the fuzzy controller

The discrete PID compensation relative coupling control designed in this paper is based on the principle of conventional relative coupling control. The discrete PID controller is introduced into the speed compensator. The basic structure of the designed discrete PID controller compensation is shown in Figure 7.

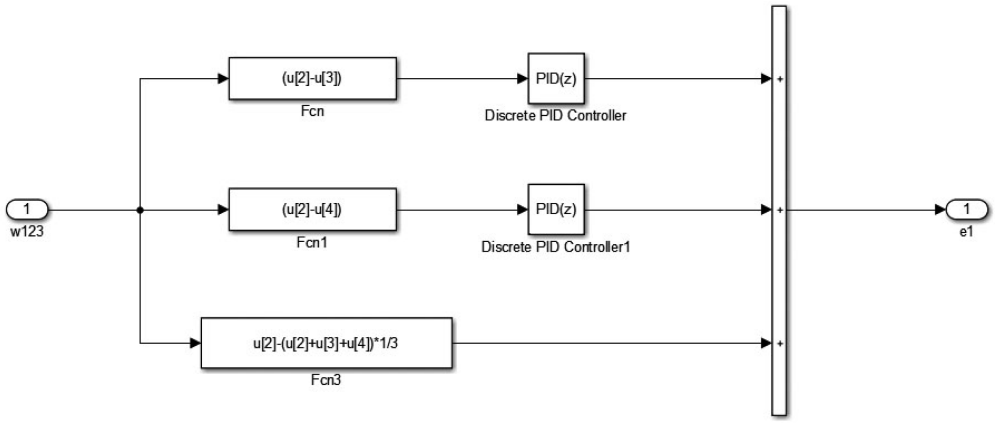

Fig. 7. Basic structure of the discrete PID controller compensation

4. Design of multi-motor neural PID deviation coupling speed synchronization control system

Based on the previous analysis of a neural PID controller and fuzzy compensation relative coupling controller, Figure 8 is the basic structure of the multi-motor neural PID relative coupling speed synchronization control system proposed in this paper.

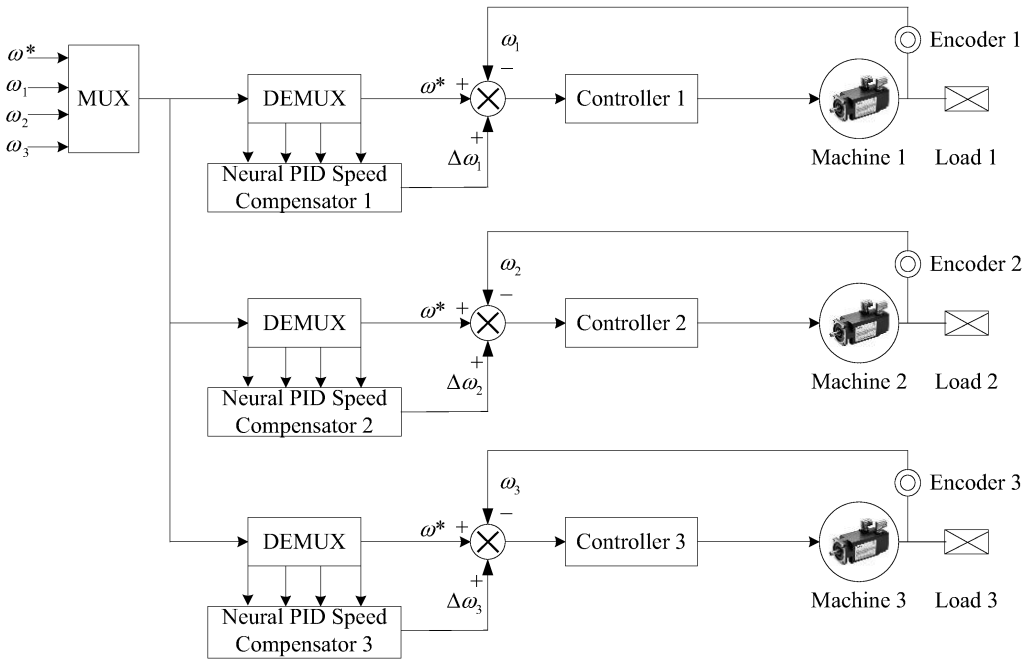

Fig. 8. Structure diagram of multi-motor neural PID relative coupling speed synchronization control system

Among them, the MUX module combines given speed and the speed of three motors, and the DEMUX module separates the combined speed signal and sends it to the speed compensator for processing to reduce tracking error and synchronization error.

5. Simulation and analysis

Based on the previous analysis, the control system proposed in this paper is built in Matlab/Simulink, and the traditional fuzzy compensation relative coupling synchronous control system and discrete PID relative coupling synchronous control system is built to form comparison. The simulation algorithm uses fixed-step ode3 with a step of $2e{-}3s$ and a simulation time of 50 s. To analyze the synchronous and anti-interfere performance of a multi motor system, at t = 5 s, t = 15 s, and t = 25 s, a disturbance load of 50 N.m (over six times of rated torque) is suddenly applied to the multi motor system. The load is shown in Figure 9.

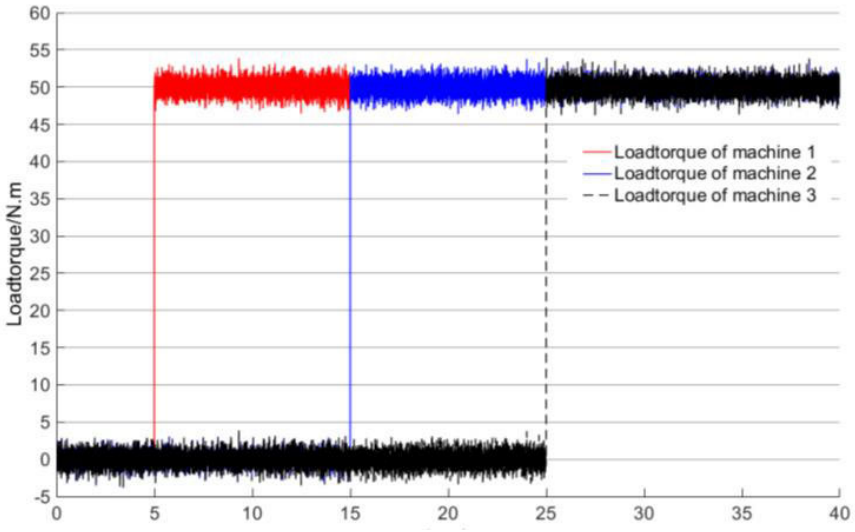

Fig. 9. Load of each motor

Figure 10 shows the operation of the three canned motors during start-up, sudden load and stable operation.

Figure 10(a) shows the operation of the three motors in the control system proposed in this paper. When one motor suddenly gets a loads, its speed drops rapidly, and the speed of the other two motors decreases and follows quickly. However, the speed of the three motors will rise rapidly within 1s and it will rise to a stable rated speed within 1.6 s.

Figure 10(b) exhibits the simulation results of the traditional fuzzy compensation relative coupling synchronous control system. Compared with Fig. 10(a), the speed of the three motors will rise rapidly within 0.75 s and it will rise to a stable rated speed within 1.2 s.

Figure 10(c) shows the results of the traditional discrete PID compensation relative coupling synchronous control system. Compared with Figure 10(a), the adjustment time is longer and more speed fluctuation during the adjustment process.

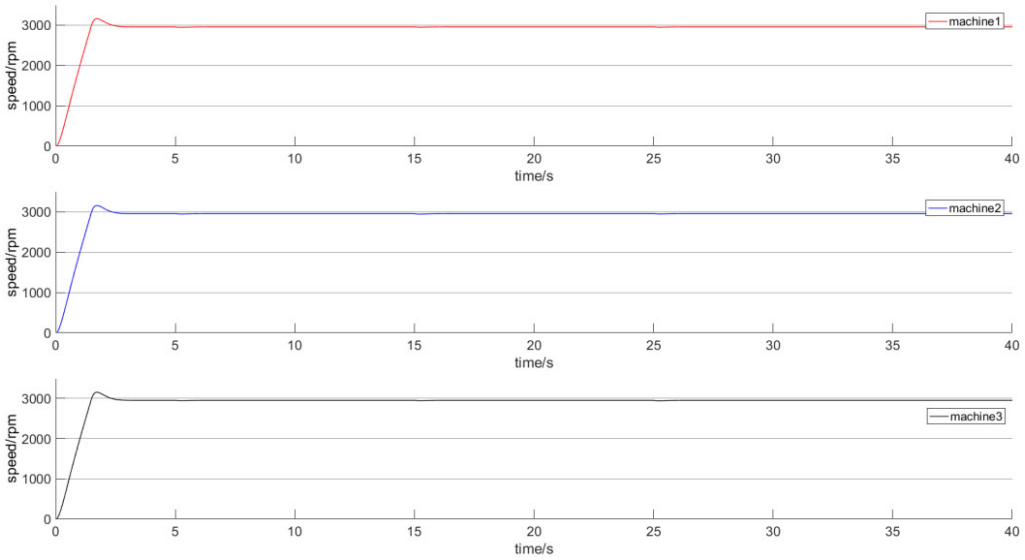

(a) Simulation results of the control system proposed in this paper

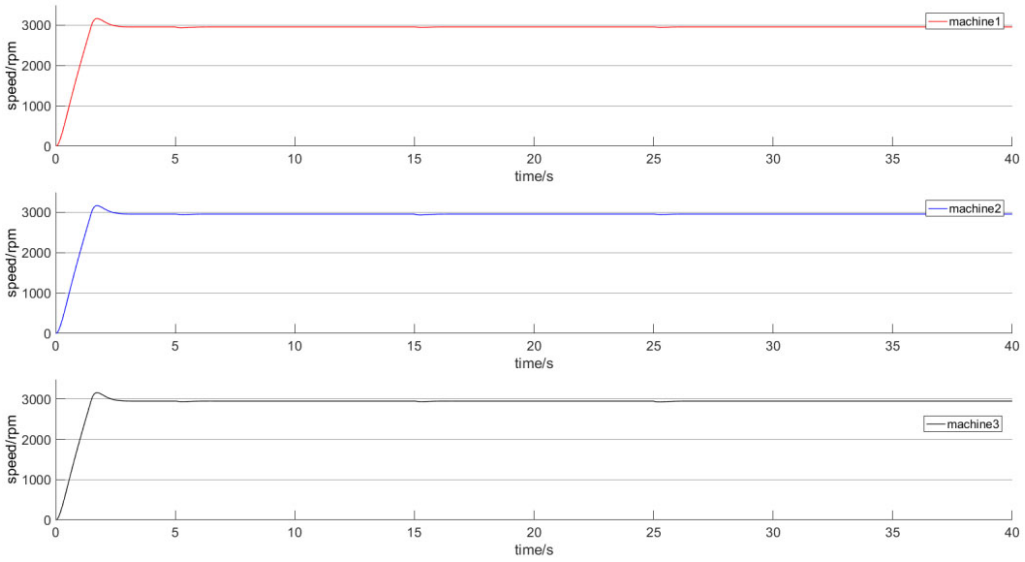

(b) Simulation results of fuzzy compensation relative coupling synchronous control

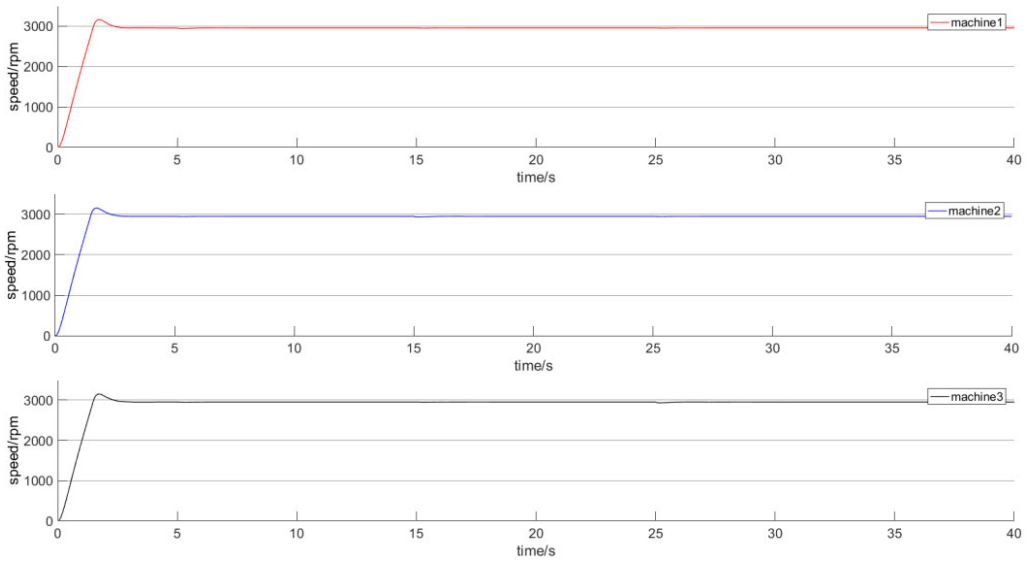

(c) Simulation results of discrete PID compensation relative coupling synchronous control

Fig. 10. Comparison of simulation results

In order to further quantitatively describe the control accuracy of the three control strategies, the speed tracking error is analyzed and compared, as shown in Figure 11.

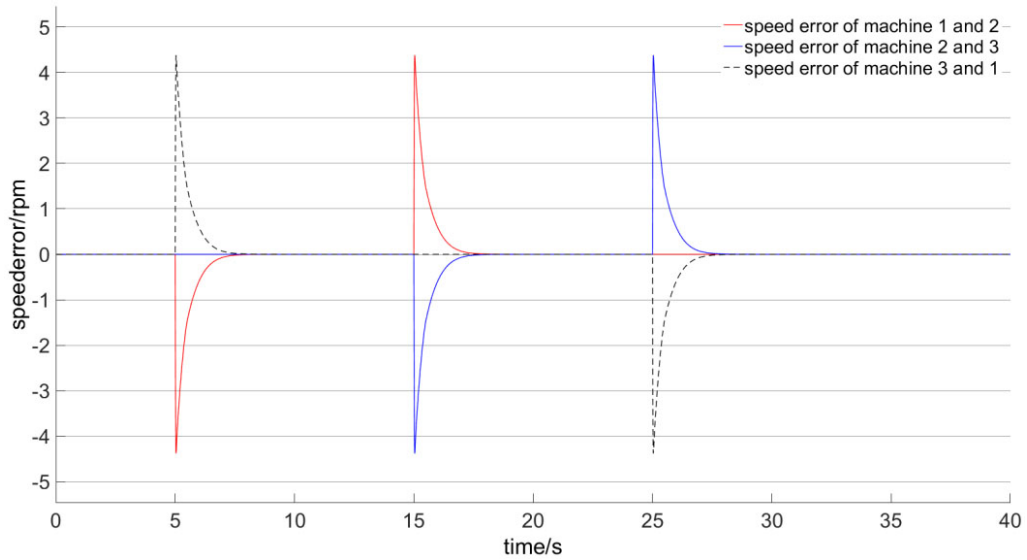

(a) Control system speed tracking error proposed in this paper

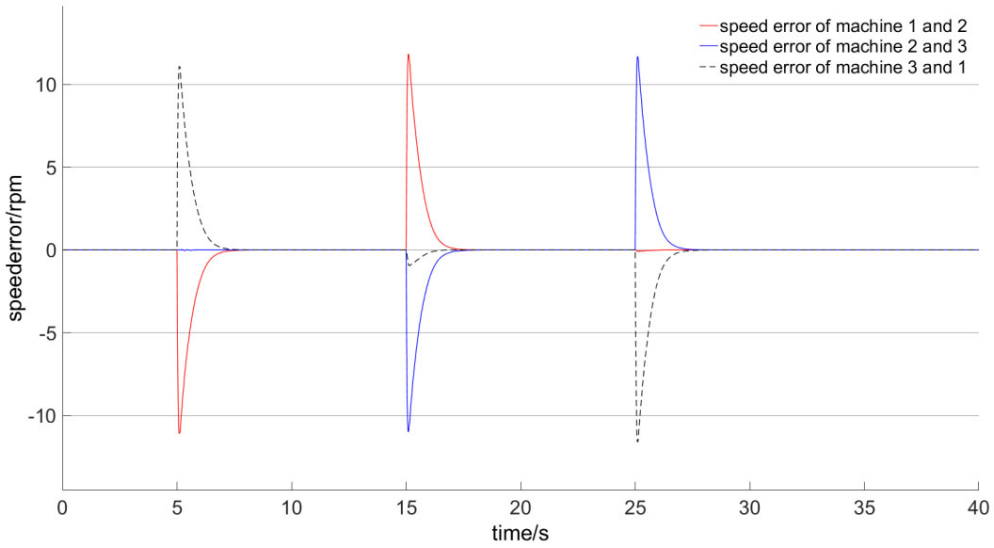

(b) Traditional fuzzy compensation relative coupling synchronous control system tracking error

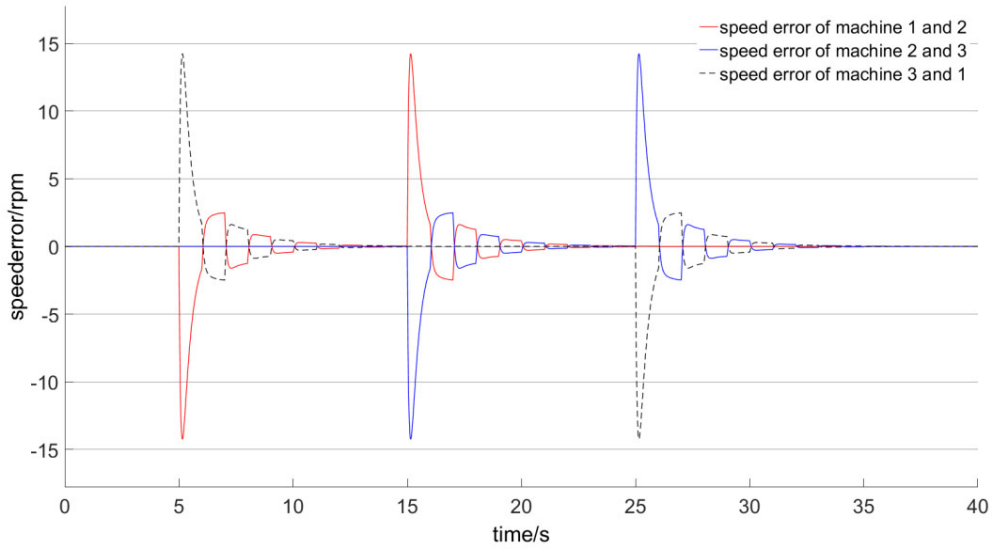

(c) Discrete PID compensation relative coupling synchronous control system tracking error

Fig. 11. Comparison of speed tracking error with different control strategy

1) The multi-motor neural PID relative coupling speed synchronous control system proposed in this paper has maximum speed error between motor 1, 2 and 3 of 4.5 rpm when the load is suddenly applied.

2) The traditional fuzzy compensation deviation coupling synchronous control system has a maximum speed error between motor 1, 2 and 3 of 10.5 rpm when the load is suddenly applied.

3) The discrete PID compensation deviation coupling synchronous control system has a maximum speed error between motor 1, 2 and 3 of 15 rpm and more speed fluctuation during the adjustment process.

In addition, we considering the different moments of inertia of the three motors, the simulation and comparative analysis of the speed synchronization error of the multi-motor synchronous control system with these different types of speed compensator.

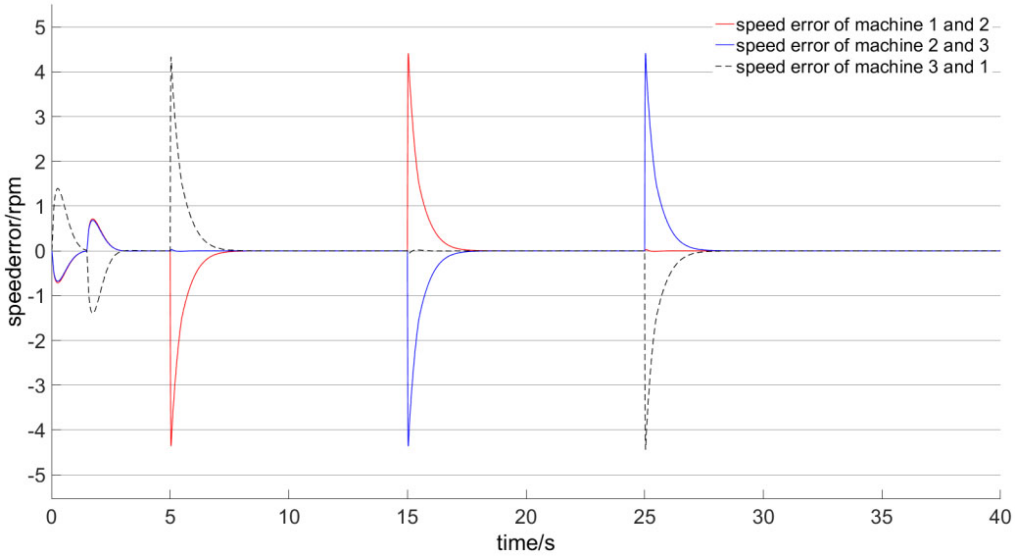

(a) Control system speed tracking error proposed in this paper

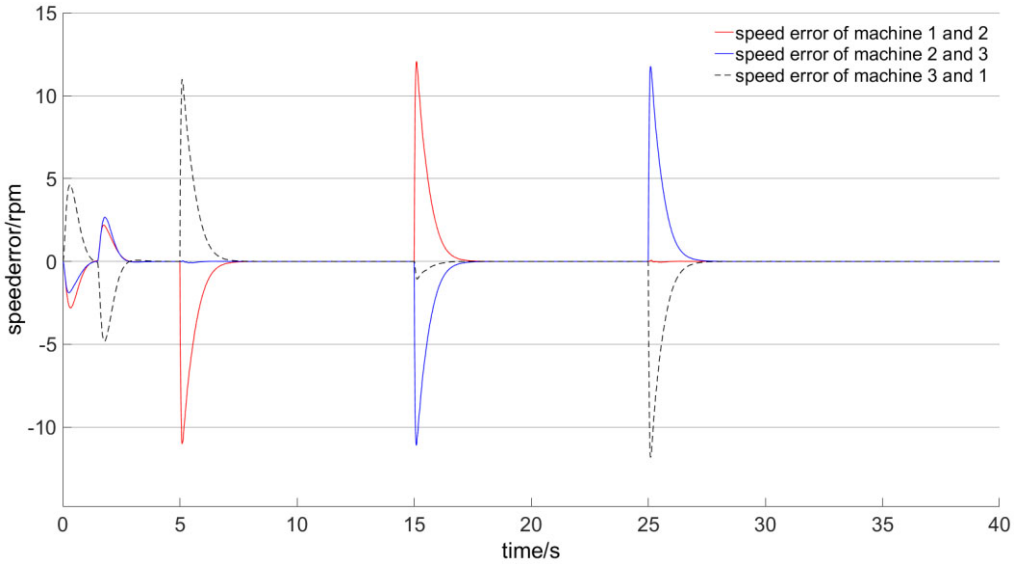

(b) Traditional fuzzy compensation relative coupling synchronous control system tracking error

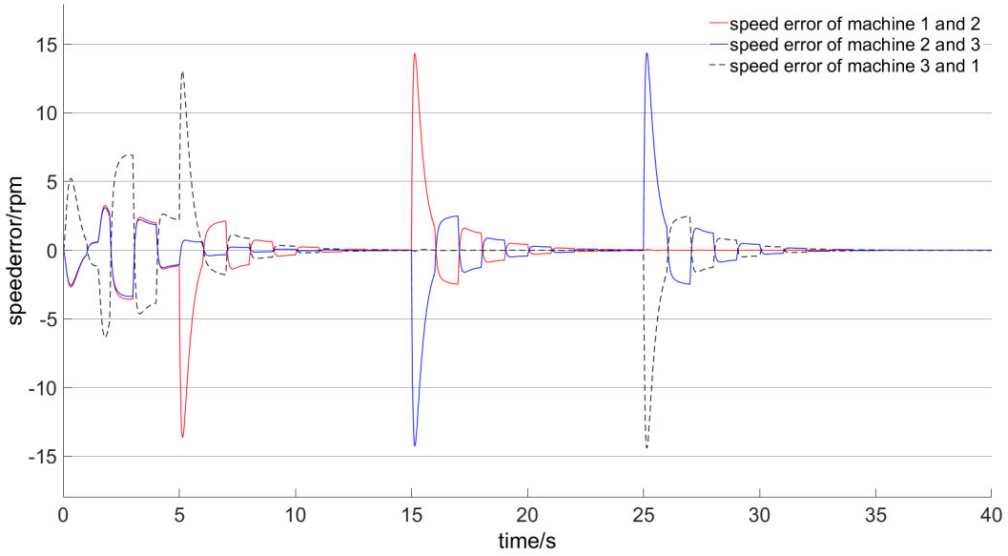

(c) Discrete PID compensation relative coupling synchronous control system tracking error

Fig. 12. Comparison of speed tracking error with different types of speed compensator under different moments of inertia of the three motors

Finally, considering the different time constants of the three motor's controllers, and keeping the other variables the same, the synchronization performance of the system is simulated and compared.

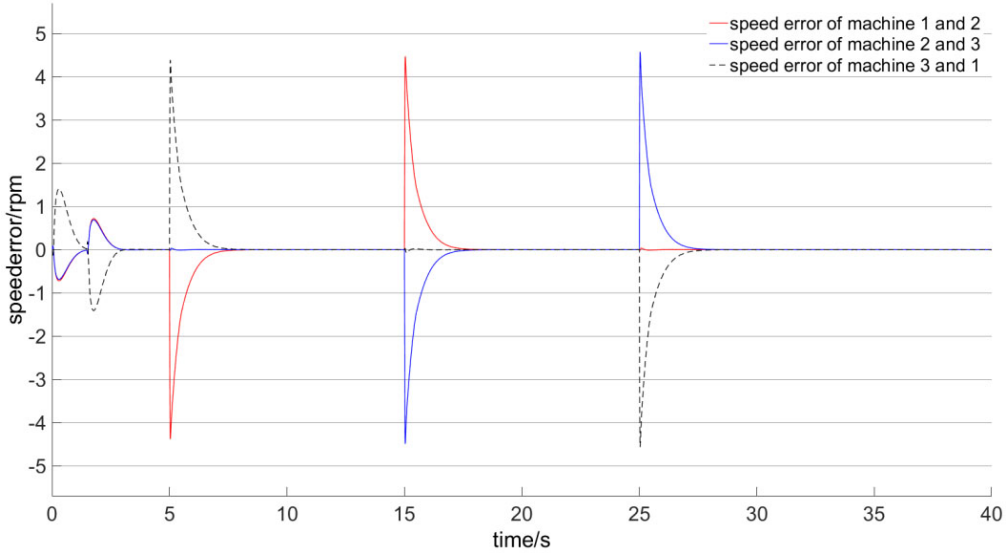

(a) Control system speed tracking error proposed in this paper

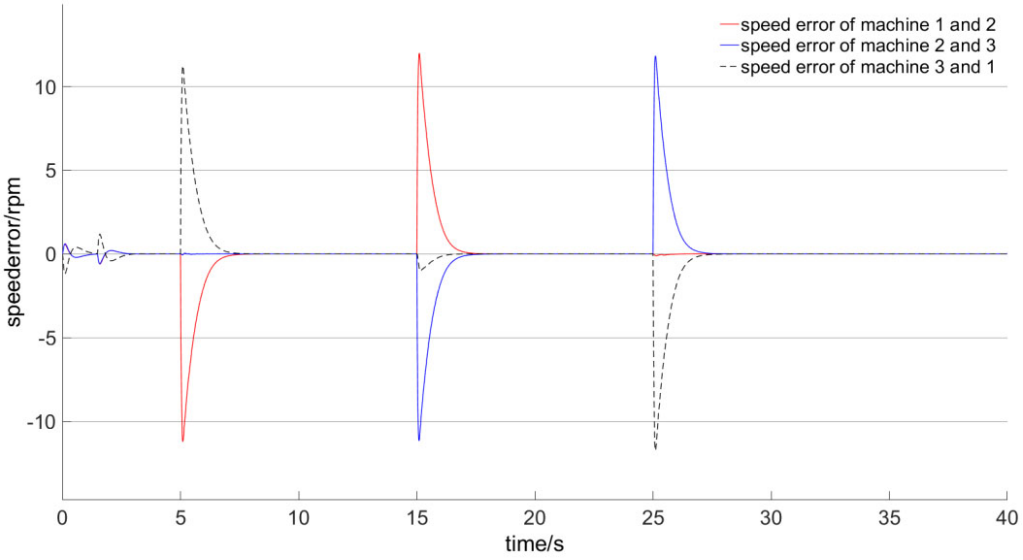

(b) Traditional fuzzy compensation relative coupling synchronous control system tracking error

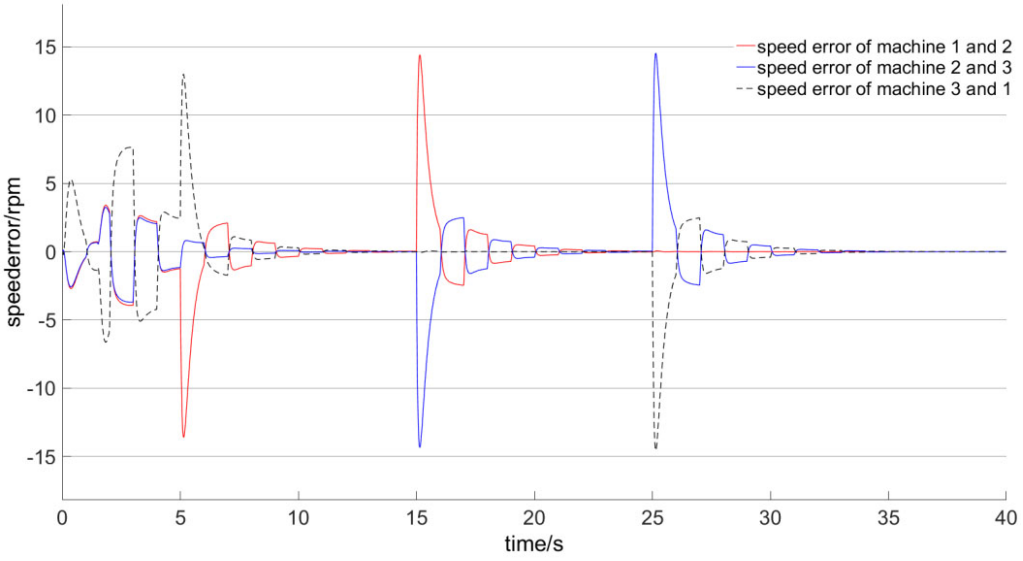

(c) Discrete PID compensation relative coupling synchronous control system tracking error

Fig. 13. Comparison of speed tracking error with different types of speed compensator under different time constants of the three motor's controllers

1) The multi-motor neural PID relative coupling speed synchronous control system proposed in this paper has a maximum speed error between motor 1, 2 and 3 of 4.5 rpm when the load is suddenly applied.

2) The traditional fuzzy compensation deviation coupling synchronous control system has a maximum speed error between motor 1, 2 and 3 of 10.5 rpm when the load is suddenly applied.

3) The discrete PID compensation deviation coupling synchronous control system has a maximum speed error between motor 1, 2 and 3 of 15 rpm and more speed fluctuation during the adjustment process.

4) As shown in Figure 12, since the three motors have different moments of inertia, although the three types of speed compensators have speed oscillations in the initial stage of adjustment, compared with the latter two schemes, the first type of system has the lowest speed oscillation and better synchronization performance.

5) In Figure 13, as the time constants of the controllers of the three motors are different, although the three types of speed compensators have speed oscillations in the initial stage of adjustment, compared with the latter two schemes, the first type of system has also the lowest speed oscillation and well synchronization performance.

6. Conclusions

In this paper, a simplified mathematical model of a canned motor is established by a transfer function. The neural network PID is introduced as a system speed compensator and a neural network PID deviation coupling speed synchronization control system is established. Theoretical analysis and simulation are compared with the control effects of typical control strategies. The results show that:

1) The multi-motor neural PID relative coupling speed synchronous control system proposed in this paper has a maximum speed error between motor 1, 2 and 3 of 4.5 rpm when the load is suddenly applied. At the same time, the synchronization error accuracy is controlled within 0.15% (speed error/rated speed).

2) Compared with the typical strategy, the maximum speed error between motor 1, 2 and 3 is reduced by 57.1%. At the same time, the synchronization error accuracy is increased from 0.36% to 0.15%.

3) Compared with the traditional control system, based on the proposed control system of this paper, reasonable topology extension can be carried out to form a multi-motor neural PID relative coupling speed synchronization control system for a vacuum pump, which has good robustness and engineering application prospects.

References

[1] Valenzuela M.A., Lorenz R.D., *Startup and commissioning procedures for electronically line-shafted paper machine drives*, IEEE Transactions on Industry Applications, vol. 38, no. 4, pp. 966–973 (2002).

[2] Lorenz R.D., Schmidt P.B., *Synchronized motion control for process automation*, Industry Applications Society Meeting (2002).

[3] Koren Y., *Cross-Coupled Biaxial Computer Controls for Manufacturing Systems* [*J*], Journal of Dynamic Systems Measurement and Control, vol. 102, no. 4, pp. 265–272 (1980).

[4] Xiao Y., Zhu K.Y., *Optimal synchronization control of high-precision motion systems*, IEEE Transactions on Industrial Electronics, vol. 53, no. 4, pp. 1160–1169 (2006).

[5] Anderson R.G., Meyer A.J., Valenzuela M.A., Lorenz R.D., *Web machine coordinated motion control via electronic line-shafting*, IEEE Transactions on Industry Applications, vol. 37, no. 1, pp. 247–254 (2001).

[6] Perez-Pinal, Nunez C., Alvarez R., Cervantes I., *Comparison of multi-motor synchronization techniques*, Conference of the IEEE Industrial Electronics Society (2004).

[7] Cong C., Liu X., Liu G., Liang Z., Li C., Zhao B., *Multi-motor Synchronous System Based on Neural Network Control*, Chinese Control Conference (2008).

[8] Liu X., *Second-order active disturbance rejection controller applied in three-motor synchronous system*, Transactions of China Electrotechnical Society, vol. 27, no. 2, pp. 179–184 (2012).

[9] Liu G., Liu P., Yue S., Wang F., *Experimental Research on Decoupling Control of Multi-motor Variable Frequency System Based on Neural Network Generalized Inverse*, IEEE International Conference on Networking (2008).

[10] Liu H., Geng Q., Xia C., Shi T., *Improved relative coupling control structure for multi-motor speed synchronous driving system*, IET Electric Power Applications, vol. 10, no. 6, pp. 451–457 (2016).

[11] Sun G., Ren X., Li D., *Neural active disturbance rejection output control of multimotor servomechanism*, IEEE Transactions on Control Systems Technology, vol. 23, no. 2, pp. 746–753 (2015).

[12] Inamura S., Sakai T., Sawa K.A, *Temperature rise analysis of switched reluctance motor due to the core and copper loss by fem*, IEEE Transactions on Magnetics, vol. 39, no. 3, pp. 1554–1557 (2003).

[13] Ergene L.T., Salon S.J., *Determining the equivalent circuit parameters of canned solid-rotor induction motors*, IEEE Transactions on Magnetics, vol. 41, no. 7, pp. 2281–2286 (2005).

[14] Tarchala G., *Sliding modes application to the control and state variables estimation of the drive system with induction motor*, Ph.D. Thesis (in Polish), Wroclaw University of Technology, Wroclaw (2013).

[15] Orlowska-Kowalska T., Tarchala G., *Sliding mode speed and torque control of the induction motor*, Electrical Engineering Review (in Polish), vol. 87, pp. 245–248 (2011).

[16] Casadei D., Serra G., Tani A., Zarri L., *Assessment of direct torque control for induction motor drives*, Bulletin of Polish Academy of Science: Technology, vol. 54, no. 3, pp. 237–254 (2006).

[17] Werner Leonhard, *Control of Electrical Drives* (2001).

[18] Zhang Y., Feng C., Li B., *Pid control of nonlinear motor-mechanism coupling system using artificial neural network*, Lecture Notes in Computer Science, vol. 3972, pp. 1096–1103 (2006).

[19] Zhongda Tian, Shujiang Li, Yanhong Wang, *T-S fuzzy neural network predictive control for burning zone temperature in rotary kiln with improved hierarchical genetic algorithm*, International Journal of Modelling, Identification and Control, vol. 25, no. 4, pp. 323–334 (2016).

[20] Zhongda Tian, *Main steam temperature control based on GA-BP optimised fuzzy neural network*, International Journal of Engineering Systems Modelling and Simulation, vol. 9, no. 3, pp. 150–160 (2017).

[21] Zhongda Tian, Gang Wang, Yi Ren, Shujiang Li, *An Adaptive Online Sequential Extreme Learning Machine for Short-term Wind Speed Prediction Based on Improved Artificial Bee Colony Algorithm*, Neural Network World, vol. 28, no. 3, pp. 191–212 (2018).

[22] Tian Z., Li S., Wang Y., Zhang Q., *Multi permanent magnet synchronous motor synchronization control based on variable universe fuzzy PI method*, Engineering Letters, vol. 23, no. 3, pp. 180−188 (2015).

[23] Zhongda Tian, Xianwen Gao, Peiqin Guo, *Network Teleoperation Robot System Control based on Fuzzy Sliding Mode*, Journal of Advanced Computational Intelligence and Intelligent Informatics, vol. 20, no. 5, pp. 828–835 (2016).

[24] Zhongda Tian, Yi Ren, Gang Wang, *Fuzzy-PID controller based on variable universe for main steam temperature system*, Australian Journal of Electrical and Electronics Engineering, vol. 15, no. 1–2, pp. 21–28 (2018).

[25] Ahmad Kalaie, Li Shujiang, Wang Yanhong, Wang Xiangdong, *Scheduling method for networked control system with resource constraints based on fuzzy feedback priority and variable sampling period*, Transactions of the Institute of Measurement and Control, vol. 40, no. 4, pp. 1136−1149 (2018).

[26] Zhongda Tian, Xianwen Gao, Dehua Wang, *The Application Research of Fuzzy Control with Self-tuning of Scaling Factor in the Energy Saving Control System of Pumping Unit*, Engineering Letters, vol. 24, no. 2, pp. 187–194 (2016).

[27] Ibrahim Z., Levi E., *A comparative analysis of fuzzy logic and pi speed control in high-performance ac drives using experimental approach*, IEEE Transactions on Industry Applications, vol. 38, no. 5, pp. 1210–1218 (2002).

[28] Ma X.J., Sun Z.Q., He Y.Y., *Analysis and design of fuzzy controller and fuzzy observer*, vol. 6, no. 1, pp. 41–51 (2002).

[29] Mirzaei A., Moallem M., Dehkordi B.M., Fahimi B., *Design of an optimal fuzzy controller for antilock braking systems*, IEEE Transactions on Vehicular Technology, vol. 55, no. 6, pp. 1725−1730 (2006).

[30] Rubaai A., Castro-Sitiriche J., Ofoli A.R., *Design and implementation of parallel fuzzy pid controller for high-performance brushless motor drives: an integrated environment for rapid control prototyping*, IEEE Transactions on Industry Applications, vol. 44, no. 4, pp. 1090–1098 (2008).